Final Report
for
Research Project T9902-27
"Streambed Simulation in Culverts"

Equilibrium Geomorphological Conditions for High Gradient Bed Steams

by

A.N. Thanos Papanicolaou
Assistant Professor

Adam R. Maxwell
Graduate Research Assistant

Principal Investigators
A.N. Papanicolaou, M.E. Barber, R.H. Hotchkiss

Washington State Transportation Center (TRAC)
Washington State University
Department of Civil & Environmental Engineering
Pullman, WA 99164-2910

Washington State Department of Transportation
Project Manager
Jim Schafer

Prepared for

Washington State Transportation Commission
Department of Transportation
and in cooperation with
U.S. Department of Transportation
Federal Highway Administration

January 2000

Disclaimer

The contents of this report reflect the views of the authors, who are responsible for the facts and the accuracy of the data presented herein. The contents do not necessarily reflect the official views or policies of the Washington State Transportation Commission, Department of Transportation, or the Federal Highway Administration. This report does not constitute a standard, specification, or regulation.

1. REPORT NO.	2. GOVERNMENT ACCESSION NO.	3. RECIPIENT'S CATALOG NO.
WA-RD 479.1		

4. TITLE AND SUBTITLE	5. REPORT DATE
Equilibrium Geomorphologic Conditions for High Gradient Bed Streams	January 2000
	6. PERFORMING ORGANIZATION CODE

7. AUTHOR(S)	8. PERFORMING ORGANIZATION REPORT NO.
A.N. Thanos Papanicolaou and Adam R. Maxwell	

9. PERFORMING ORGANIZATION NAME AND ADDRESS	10. WORK UNIT NO.
Washington State Transportation Center (TRAC) Civil and Environmental Engineering Sloan Hall, Room 101 Washington State University Pullman, Washington 99164-2910	11. CONTRACT OR GRANT NO. T9902-27

12. SPONSORING AGENCY NAME AND ADDRESS	13. TYPE OF REPORT AND PERIOD COVERED
Research Office Washington State Department of Transportation Transportation Building, MS 7370 Olympia, Washington 98504-7370 Jim Schafer, Project Manager, (360)705-7403 Paul Wagner, Technical Monitor	Final Report
	14. SPONSORING AGENCY CODE

15. SUPPLEMENTARY NOTES

This study was conducted in cooperation with the U.S. Department of Transportation, Federal Highway Administration.

16. ABSTRACT

The goal of this study was to identify the flow conditions under which stable bedforms exist; provide the geometric characteristics of these bedforms; measure the magnitude of the streamwise velocity and energy dissipation factor; and determine the friction factor under various flow conditions and gravel sizes. Design criteria and recommendations for stable bedforms were provided upon the termination of this research. Stable bedforms are defined as those bedforms of which the spatial characteristics (height and spacing) do not change with time. The focus of this study was on streams with slopes greater than the 3%, as clear design requirements for bed geomorphologic stability are lacking for these cases, and are of particular interest in design and retrofit of culverts for both anadromous and resident migratory fish passage.

17. KEY WORDS	18. DISTRIBUTION STATEMENT
Key words: Step-pools geomorphologic characteristics, frictional characteristics, bed failure conditions, hydraulics characteristics for high gradients bed streams	No restrictions. This document is available to the public through the National Technical Information Service, Springfield, VA 22616

19. SECURITY CLASSIF. (of this report)	20. SECURITY CLASSIF. (of this page)	21. NO. OF PAGES	22. PRICE
None	None		

TABLE OF CONTENTS

Acknowledgements

The researchers and WSDOT gratefully acknowledge the technical assistance and support from the Salmon Research Advisory Committee, and especially the contributions of the following people during the planning, development, and execution of this project:

Ken Bates	Washington State Dept. of Fish and Wildlife
Pat Powers	Washington State Dept. of Fish and Wildlife
Bob Barnard	Washington State Dept. of Fish and Wildlife
Bruce Heiner	Washington State Dept. of Fish and Wildlife
Larry Cowan	Washington State Dept. of Fish and Wildlife
Chris Katopodis	Canadian Dept. of Fisheries of Oceans
Pat Syms	Technician, Washington State University
Rob Hilldale	Tech Assistant, Washington State University

1. Introduction-Objectives

The objective of this investigation was to explore the geomorphologic characteristics of streams with steep gradient (i.e., streams with slope greater than 3%) and identify the hydraulic conditions under which stable geomorphologic characteristics form. There are several bed formations (called bedforms) present in steep-slope streams, namely, pool-riffle at small slopes (0.2-1%); plane bed at intermediate slopes (1-3%); and step-pool at slopes greater than 3%.

In order to provide quantitative measures about the spatial and temporal characteristics of these bedforms, a pilot laboratory study was performed at the facilities of Washington State University. The goal of this study was to identify the flow conditions under which stable bedforms exist; provide the geometric characteristics of these bedforms; measure the magnitude of the streamwise velocity and energy dissipation factor; and determine the friction factor under various flow conditions and gravel sizes. Design criteria and recommendations for stable bedforms were provided upon the termination of this research. Stable bedforms are defined as those bedforms of which the spatial characteristics (height and spacing) do not change with time. The focus of this study was on streams with slopes greater than 3%, as clear design requirements for bed geomorphologic stability are lacking for these cases.

This study was performed in a tilting, water recirculating flume that is 70 ft long, 3 ft wide and 2 ft deep (See photos in Appendix A). The flume recirculates water at a rate of up to 13 cubic feet per second (cfs) and can be tilted up to 14%. To evaluate the bed forms encountered in gravel bed streams, three sets of experiments were performed. The first set was performed when the gravel characteristic diameter D_{84}=2 inches; the second experiment was performed with D_{84}=4 inches; and the third with D_{84}=6 inches. To ensure that the laboratory tests do not violate the laws of dynamic similarity for flow and gravel (sediment), an integrated dynamic similarity approach was developed. This integrated approach allows the user of this method to "scale-back" the laboratory data to (real) field conditions and vice versa. The scaling approach used here has two components: scaling for the flow and culvert used in this study; and scaling for the gravel. For all cases, the Froude number similarity approach was used. Traditionally, the scaling of sediment is conducted by using the particle Reynolds number similarity; however, the researchers of this investigation have clearly postulated that for steep streams the Reynolds number similarity is not valid since gravity becomes more dominant than the viscous forces. Hence, the particles are scaled according to the dimensionless shear stress parameter. The equations of dynamic similarity approaches are included in this report in a manner that can be easily applied. The similarity approach is a vital part of this investigation.

The following methodology was established during the tests:

1). For a fixed gravel size configuration and slope, experimental runs were performed for different flow conditions to identify the conditions under which bed failure occurred; relative submergence (the relative submergence is defined as the ratio depth:D_{84}) varied from 0.75 – 2.50, depending on bed stability. Each run was performed for several minutes or hours depending on the outcome and peculiarity of the tests. When the stable geomorphologic conditions were determined, the test was terminated. Surveying at the termination of each test was performed to obtain the height of the pools formed along the flume bed and the frequency of spacing among pools.

2). For the stable configuration, determined in step 1, velocity measurements were performed for depth:D_{84} ratios equal to 0.5 and 1.0. These are the projected conditions, under which fish will utilize culverts as fish passages.

3). Measurements of the average depth velocity in the longitudinal and transverse directions were obtained for each experimental case by means of a velocity probe (Swoffer current meter). It was not possible to collect turbulent measurements, due to the low-flow depth conditions present in the tests. However, conclusions/speculations about the level of turbulence were made for all tests.

4). Corrections of the flow measurements made via Swoffer were performed to match the velocity magnitudes calculated from the flow-gauge devices attached to the flume. The correction is applied based on a best-fit between the Froude number based on the Swoffer meter vs. the Froude number based on the calculated velocity (from continuity).

The outcome of this study consists of several unique findings:

It was verified that for slopes greater than 3% the dominant bedform-feature in gravel bed streams, for the sizes examined here, is the step-pool feature. Similar conclusions have been reached by other researchers (e.g., Billi et al. 1999).

1. A dimension-less equation was derived to provide the height of the pools as function of discharge, depth, slope, and geometric standard deviation. This relationship is valid when stable bedforms are formed.

2. The spacing of the pools was determined. For this purpose, a formula was provided.

3. The magnitude of the velocity and of the energy dissipation value was determined for the model.

4. For each case, the critical unit discharge was calculated by using the Bathurst et al. (1987) formula.

5. The friction factor was determined. The friction factor values appear to be evenly divided in a close agreement with those provided by the Bathurst et al. (1985) method and the Rice et al. (1998) formula.

6. An example was provided illustrating the scaling method and use of the above results.

2. Critical review of the literature

a. Resistance to flow

As soon as sediment particles enter motion, the random patterns of erosion and sedimentation generate very small perturbations of the bed surface elevation. In many instances, these perturbations grow until various bedforms cover the entire bed surface. Resistance to flow, which depends to a great extent on bed form configuration, directly affects water surface elevation in mountain streams.

Estimation of the flow resistance in open channel flows is essential. Traditionally, flow resistance is predicted by means of the Manning and Darcy-Weisbach equations. Because these equations were developed for uniform and steady flows their use in non-uniform and unsteady flows (typically encountered in mountain streams) is questionable.

Several researchers have proposed different equations to measure the Darcy-Weisbach friction coefficient or the Manning's roughness coefficient. Jarrett (1984) for slopes within the range of 0.002-0.04 developed the following equation,

$$n = 0.39 S_f^{0.38} R^{-0.16} \quad (1)$$

where S_f is the friction slope and R denotes the hydraulic radius in ft.

Bathurst (1985) using data for rivers with slopes of 0.004-0.04 developed a relationship for estimating the resistance of flow in terms of the Darcy-Weisbach friction factor:

$$\left(\frac{8}{f}\right)^{1/2} = 5.62 \log\left(\frac{H}{D_{84}}\right) + 4 \quad (2)$$

H denotes the average flow depth in a cross-section and the ratio $\frac{H}{D_{84}}$ is known as the relative submergence ratio. Abt et al. (1987) provided a relationship for slopes ranging from 0.01 to 0.20 for the Manning's roughness coefficient, for D50 in in.:

$$n = 0.0456 (D_{50} S)^{0.159} \quad (3)$$

Ugarte and Madrid (1994) developed an expression for n for large-scale roughness:

$$n = [0.183 + \ln(1.7462 S_f^{0.1581} / F_d^{0.2631})]\left(\frac{D_{84}^{1/6}}{g^{1/2}}\right) \quad (4)$$

where F_d is the Densimetric Froude number and g is the acceleration of gravity. Finally, Rice et al. (1998) proposed the following friction factor on slopes varying from 2.8% to 33%.

$$\left(\frac{8}{f}\right)^{1/2} = 5.1\log\left(\frac{H}{D_{84}}\right) + 6 \qquad (5)$$

What is missing from the above theory?

Despite the progress that has been made in the flow-resistance theory, most of the equations found in the literature are of a limited use in this study.

The Rice et al. (1998) formula has been developed for steep-slopes, however, the sediment used in their study was of an angular shape (here the shape is rounded). Thus, any direct use of this formula in this study is not appropriate.

Bathurst's formula (1985) is limited to slopes of magnitude less than the magnitude examined (otherwise, this formula could be used directly in this research). Use of this equation is not suggested for slopes greater than 4%.

In the present study a new formula applicable for rounded gravel and for slopes varying within the range of 3% to 9% is suggested. A comparison between the formulas developed here and those of Rice et al. (1998) and of Bathurst (1985) is provided.

Moreover, the friction coefficient f is calculated based on the definition of the Darcy-Weisbach friction factor for open channel flows. Moreover, the scaling of the sediment properties is not determined via the Manning equation since this equation is not in general applicable for non-uniform flows.

b. Mesoscale-Bedforms for Mountain streams

In mountain streams three distinct mesoscale bedforms typically occur (Billi et al. 1998);

1. the pool-riffle sequence for gravel rivers for slopes less than 5 per cent (Sear 1996)
2. the mixed mesoscale sequence (occurrence of clustering-grouping of gravel and pool-riffle sequence)
3. the step-pool sequence for slopes greater than 7.5 per cent (Whittaker and Jaeggi 1982).

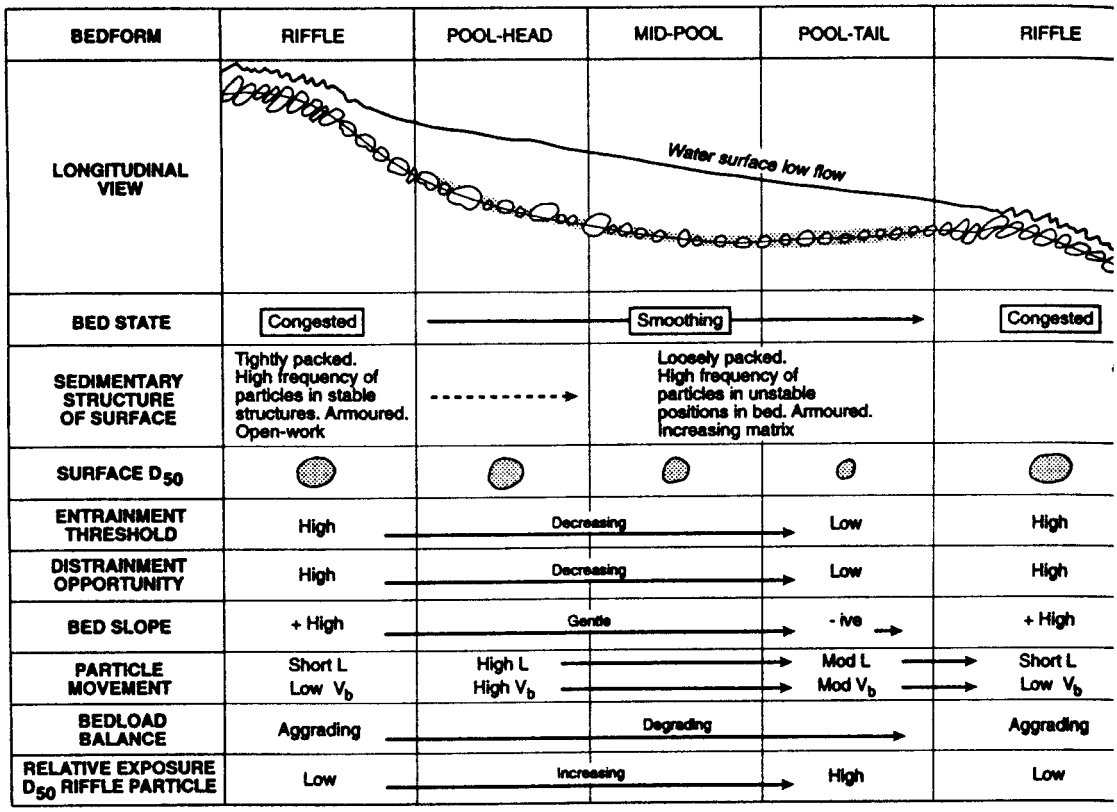

Figure. 1 Variation of sediment size within a pool.

The pioneers in the field of step-pool bedforms are: Whittaker and Jaeggi (1982), Grant et al. (1990), and Billi et al. (1998). According to the above, L_p obtains values within the range of 1.2 to 10.2 cm. Billi et al. (1999) suggested that the spacing L between the summits of two subsequent steps is well described by the following relation:

$$L = 0.806\ L_p + 1.06 \qquad (6)$$

Where L_p is defined in Figure 2 as the spacing between consecutive pools. Note that L and L_p in (6) are expressed in meters.

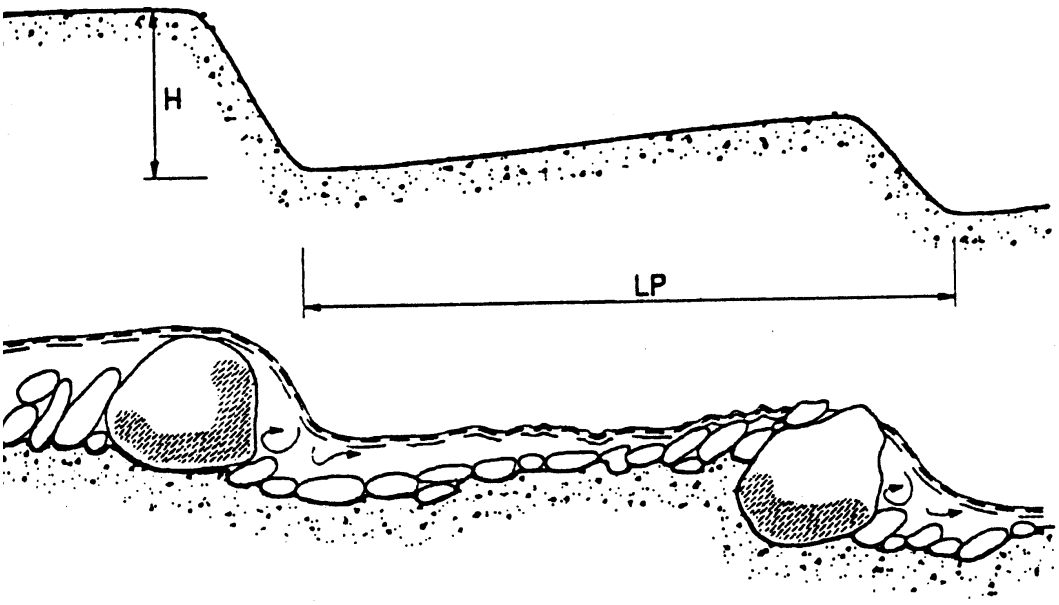

Figure 2. Step-pool sequence, after Billi et al. (1998)

While the above slope ranges are generally accepted by many for defining the different bed forms in gravel bed streams, there are several other conflicting reports related to the slope conditions under which bed forms for gravel form. According to Lopez and Falcon (1999) and Montgomery and Buffington (1993), pool-riffles occur at small slopes (0.2-1%); plane bed occur at intermediate slopes (1-3%); and step-pool form at slopes greater than 3%.

What is missing here?

The above suggest that there is some controversy on the range of slope values under which the above bed features appear to form. Because bed forms are important features that influence flow turbulence and affect fish habitat, the present investigation will attempt to identify the slope conditions under which these bed forms occur. A comparison between the aforementioned studies with this study will be provided.

c. Stability criteria

Several approaches have been presented for predicting stability of sediment motion in steep channels with shallow flows. The most common approach is to relate the dimensionless critical shear stress to the relative depth, H/D_{50}.

Ashida and Bayazit (1973) ran a set of experiments in a tilting flume using natural gravel. The relative depth in this set of

experiments ranges from 0.6 to 8.5. Shields' approach of extrapolation to zero transport was used as a criterion for threshold conditions. The results show that the dimensionless critical shear stress increases considerably as the flow becomes shallower. In fact, τ_{cr}^* for the lowest relative depth in the range turns out to be over 3 times higher than the τ_{cr}^* corresponding to the highest relative depth.

Mizuyama (1977) used this data as well as data from Tabata and Ichinose (1971) to develop an empirical expression for the dimensionless critical shear stress as a function of relative depth. It was suggested that for $H/D_{50} \geq 4.55$, $\tau_{cr}^* = 0.04$. This might indicate that the traditional Shields diagram can be used to predict the initiation of sediment motion at relative depths greater than 4.55. However, caution must be exercised because the data show some scatter. For $H/D_{50} \leq 4.55$, the empirical expression is

$$\tau_{cr}^* = 0.034 \times 10^{0.32\frac{D_{50}}{H}} \qquad (7)$$

Suszka (1991) studied the same type of relationship using gravel-bed flume data from 5 sources. The Pazis and Graf (1977) probability-concept was used as the criterion for incipient conditions. The range of relative depths in this data set (H/D_{50} = 1.2-50) is considerably wider than the Ashida and Bayazit range. The two data sets follow the same general trend. Slight

differences can be explained by the different criterion for threshold conditions used. Suszka's data points indicate that the traditional Shields diagram can be used for relative depths greater than 10, approximately.

Suszka used the data to express τ_{cr}^* as a power function of relative depth as follows

$$\tau_{cr}^* = 0.0851\left(\frac{H}{D_{50}}\right)^{-0.266} \qquad (8)$$

Bathurst et al. (1985) did a similar analysis using their incipient motion data as well as that of several other investigators. In addition, they looked further into the effect of slope, S. Their analysis indicated that for flows with $S \leq 1$ %, the dimensionless critical shear stress varies gradually and remains between 0.04-0.06 as in the Reynolds number independent region of the traditional Shields diagram.

In a similar approach, Graf and Suszka (1987) used their own data as well as data from Cao (1985) and Mizuyama (1977) to study the effect of slope on the dimensionless critical shear stress. The highest slope in this data is about 20 %. Based on this study it is evident that for particle Reynolds numbers greater than about 500, the Shields parameter is dependent on the slope. The relation fitted to the data is

$$\tau_{cr}^* = 0.042\left(10^{2.2S}\right) \qquad (9)$$

This data also shows that for $0.005 < S < 0.025$ the average value of τ_{cr}^* is 0.045. The upper limit of the slope (S = 2.5 %) for obtaining this constant Shields parameter is considerably higher than that given by Bathurst et al. (S = 1 %). The value of τ_{cr}^* given by Graf and Suszka is also within the bounds usually obtained in the Reynolds number independent region of the Shields diagram. It must be pointed out that τ_{cr}^* in this region is considerably lower when dealing with fully exposed spherical particles. Fenton and Abbott (1977) and Coleman (1967) obtained values close to 0.01 for this case.

Discussion related to stability criteria

So far in this discussion, data from a variety of sources have shown that τ_{cr}^* increases with decreasing relative depth in shallow flows. Data obtained from a Chinese river by Li (1965) show the opposite effect. This limited set of data has a relative depth range of 6.5-9.25. Interestingly enough, $\tau_{cr}^* = 0.153$ at $H/D_{50} = 6.5$ and $\tau_{cr}^* = 0.326$ at $H/D_{50} = 9.25$. Wang and Shen (1985) analyzed this data along with another set of data from Chinese rivers reported by Wang (1975). The relative depth for all the Wang data is around 10 and a best-fit line shows that $\tau_{cr}^* = 0.062$. According to Wang and Shen, the cause for the dramatic increase of τ_{cr}^* in Li's data is caused by the significant reduction in the drag coefficient, C_D, that occurs at Reynolds numbers between 10^4 and 10^5). The main drawback of Li's

data is that it is very limited. Also, it is more difficult to have a clear definition of incipient conditions in the field than it is in a laboratory flume. Finally, Wittler and Abt (1995) commented that the experiments analyzed by Wang and Shen were affected by aeration just like the Abt et al. (1988) tests.

The various formulae and expressions should be applied with caution when designing stable bed forms. Before using one of them, one must look into how that particular relationship was developed. First, natural gravel was used and this most closely resembles riprap. Second, the data comes from a variety of sources and seem to agree well with each other. Finally, the fact that $\tau_{cr}* \approx 0.04$ in the Reynolds number independent region shows that these results agree well with those in well-known publications. **A safety factor of (1.2) must always be applied because scatter is present when dealing with incipient motion criteria.**

Another approach for predicting the initiation of motion in mountain rivers with shallow flows is by relating the Shields parameter ($\tau_{cr}*$) to the Froude number. Kilgore and Young (1993) collected data from a variety of sources plotted $\tau_{cr}*$ vs. Froude number. This plot shows that a strong correlation exists between the dimensionless critical shear stress and the Froude number. For flows with Froude number less than about 0.4, $\tau_{cr}*$ is approximately equal to 0.05, which is in between the values of

0.04-0.06 typically obtained in the Reynolds number independent region of the traditional Shields diagram. At Fr > 0.4, τ_{cr}^* increases as the Froude number increases. **Kilgore and Young suggest that the traditional Shields diagram should not be used to design riprap for flows with Froude number greater than 0.8.** The following empirical expression, which is valid for any Froude number, was developed:

$$\tau_{cr}^* = 0.052 Fr^{2.7} + 0.05 \qquad (10)$$

The advantage of this expression is that it is based on data from several well-known sources and the scatter is not significant. However, some values of τ_{cr}^* in this data set might be too high. More than 10 points have a dimensionless critical shear stress that exceeds 0.15. In comparison, the highest values of τ_{cr}^* obtained by Ashida and Bayazit (1973), Suszka (1991), and Bathurst et al. (1982) are 0.1178, 0.098, 0.108, respectively. The Kilgore and Young equation tends to over-predict the dimensionless critical shear stress. For example, a data point from the Bathurst et al. (1982) data with a Froude number of 1.23 has a τ_{cr}^* value of 0.108. According to equation 10, the shear stress is 0.141. The high values of τ_{cr}^* obtained by Kilgore and Young can be explained in part by the use of Wang and Shen's (1985) data, which has raised some questions as mentioned earlier. Suszka's data is not included because he provides no information on velocity. The data points from the Bathurst et al. and Ashida and Bayazit analyses have a significant amount of

scatter. One possible explanation is that the Froude numbers from the Ashida and Bayazit study were calculated using a depth averaged velocity based on the flow rate. This might not be an accurate velocity because the slopes and Froude numbers were very high and the flow depths very low. The presence of surface waves and possible aeration make the velocity difficult to measure accurately.

This section will end with a short discussion on the highest Froude numbers that are to be expected in natural channels. Based on personal communication with other modelers and years of experience, Trieste (1992) commented that few situations arise where supercritical flow exists along a channel reach longer than 7.6 m. Bathurst (1978) noted supercritical flow in a very limited areal extent. Field data collected by Jarrett (1984) with slopes as steep as 5.2% indicate that all flows were sub-critical. After reviewing data from 433 gauging stations in Colorado, Wahl (1993) indicated that very few flows were supercritical. These authors agree that supercritical flow appears in small reaches of high-gradient channels, but quickly changes back to sub-critical because of extreme energy dissipation and turbulence due to obstructions. Bathurst et al. (1979) also showed that additional energy is consumed when bed material is transported. Even though few situations revealed supercritical flow, Jarrett and Wahl’s data indicate that a significant number of flows in natural channels have Froude numbers between 0.7 and 1.0. As shown by

Kilgore and Young's data, there is a strong relationship between τ_{cr}^* and the Froude number in that range.

In the present study several of the above stability criteria were employed and compared with the criteria determined experimentally here. A comparison of these data is provided in the results section.

3.Experimental set-up

The tests were performed in the Albrook Hydraulics Laboratory of Washington State University. The primary test apparatus was a water re-circulating, tilting flume. This flume is 70 feet long, 2.9 feet wide, and has a usable depth of 1.7 feet. It is capable of attaining slopes of up to 14%, by means of screw jacks. The floor and one wall of the flume are lined with opaque PVC sheets, while the remaining side is Plexiglas, which enables side viewing of the flow. The headbox of the flume is equipped with a honeycomb structure, which provides rectilinear flow, minimizing the surface effects caused by air bubbles in the piping.

Several pumps were available for use. For testing at low flow-rates, one or both of two Scot 7.5 HP pumps were used, which provide 1 cubic foot per second (cfs) each. One of the pumps is equipped with a simple on/off toggle, while the other is governed by a frequency inverter, which allows motor RPM to be infinitely variable. Flow rate through these pumps is measured with a Venturi and mercury-water manometer. For slightly larger flow

requirements, an additional 5 HP pump was used, which is equipped with a magnetic flow meter; this pump produces 0.73 cfs. The majority of the tests, however, were performed using a 40 HP, 2-stage Johnston propeller pump, rated at 12 cfs. The flow from this pump is regulated using a gate valve and pressure bypass, and flow rate is measured using a solid-state magnetic flow meter and digital frequency counter. All of the pumps draw from a large, semi-enclosed sump, located under the flume and the floor of the facility.

The culvert used, **donated by Advanced Drainage Systems**, was of a corrugated plastic type. The inner wall of the culvert was smooth, except for shallow annular corrugations (depth not measurable). This was desirable so as to minimize the effects of the wall corrugations on the water velocity, as these effects would have extended disproportionately into the flowstream of the model, vs. the prototype culverts under consideration. The inside diameter (ID) of the culvert was 2.5 feet, and the outside diameter (OD) was 2.9 feet wide, eliminating the necessity of building a cradle in the flume to support the culvert. The culvert was assembled from two 20 foot long sections, each equipped with a male and female (bell) end. The downstream culvert section was placed 12 feet from the outlet of the flume, in order to avoid outlet scour due to the local accelerations at the flume terminus. This placement also allowed sufficient distance to establish flow upstream of the culvert.

Inlet and outlet plates were constructed to prevent the flow from passing along the sides of the culvert, while allowing flow to continue unrestricted through the culvert. Lightweight concrete, using a perlite aggregate, was formed on wire mesh at the inlet and outlet, ensuring a streamlined transition; rubberized paint was used to ensure durability of the concrete.

To protect against massive erosion of the culvert bed, in case of total bed failure, control sills were placed at approximately 1 foot intervals along the bottom of the culvert; these consisted of a bar of PVC, placed in the horizontal plane and secant to the culvert diameter, approximately 1 inch from the bottom of the culvert.

To minimize the dead weight loading in the flume, due to the large volume of gravel required, dense insulating foam, known as "pink board," was placed on the bottom of the flume, upstream and downstream of the culvert. U-shaped bands were manufactured to prevent these from floating, as this occurred during an initial trial. A single, 8 foot section of pink board was also placed on each side of the flume, upstream and downstream of the culvert, to minimize the effects of the contraction and expansion caused by the culvert inlet and outlet, respectively. To capture the sediment as it moved toward the outlet of the flume and to measure bedload rate a sediment trap was placed at the downstream end of the flume.

The following tests were conducted throughout the course of this investigation.

Table 1. Experiments performed in this study

D_{84}	S (%)	Testing Procedure
2.5"	3	TEST 1 - Begin test at H/D_{84} = 1.0 (+- 0.2). Increase the flow until the bed structure forms but does not fail. If the bed fails go to next D_{84}. If bed is stable, measure hydraulic parameters at H/D=1.0, and 0.5 (by decreasing the flow). Then increase the flow to H/D = 2.0. If the bed fails go to the next slope. If the bed is stable, measure the hydraulic parameters and then proceed to next slope.
	5	TEST 2 - Same as above
	7	TEST 3 - Same as above
4.0"	3	TEST 4 - Begin test at H/D_{84} = 1.0 (+- 0.2). Increase the flow until the bed structure forms but does not fail. If the bed fails go to next D_{84}. If bed is stable, measure hydraulic parameters at H/D=1.0, and 0.5 (by decreasing the flow). Then increase the flow to H/D = 2.0. If the bed fails go to the next slope. If the bed is stable, measure the hydraulic parameters and then proceed to next slope.
	5	TEST 5 - Same as above
	7	TEST 6 - Same as above
	9	TEST 7 - Same as above
5.0"	5	TEST 8 - Begin test at H/D_{84} = 1.0 (+- 0.2). Increase the flow until the bed structure forms but does not fail. If the bed fails go to next D_{84}. If bed is stable, measure hydraulic parameters at H/D=1.0, and 0.5 (by decreasing the flow). Then increase the flow to H/D = 2.0. If the bed fails go to the next slope. If the bed is stable, measure the hydraulic parameters and then proceed to next slope.
	7	TEST 9 - Same as above
	9	TEST 10 - Same as above
	11	TEST 11 - Same as above

Before data is measured to complete a test, bed must be stable for 12 hours. If there is no bed alteration wihtin 1 hour, increase the flow to the next H/D. Note: H/D values are approximate. The model flow rate does not need to be fine tuned to meet the exact values.

Trial-and-error tests were conducted and documented, to establish a reliable testing procedure and eliminate errors in the process. Several operational issues arise in testing a mobile-bed model of this type (marginal transport rate is allowed); one example is the question of the rate of increase of the model inflow. If the flow is increased rapidly, the bed will scour immediately as the

wave of water passes over it. A rate of increase must be found which establishes flow in a reasonable amount of time, while still preventing scour.

One problem encountered was that the local acceleration of the free-falling flow at the outlet of the flume caused scour downstream of the culvert. This in turn caused artificial erosion rates upstream, in a demonstration of Lane's well-known relationship between sediment load, sediment size, flowrate, and stream slope; namely, that $Q_s D_s \bullet QS$ (Chang, 1988). This problem was alleviated by the use of a V-notch weir as a sluice gate at the flume outlet, which allowed sediment to pass the end of the flume. The use of the weir as a sluice added another adjustment to the flume operating condition, however, as its height must be increased or decreased in direct proportion to the flowrate to prevent either massive erosion of sediment or overtopping of the flume sidewalls.

The basic testing procedure was as follows, for a given sediment size distribution:

1. Flatten bed, mix sediment
2. Set slope at 3%
3. Survey centerline of flat bed
4. Run water at depth of $H/D_{84} = 0.5$ or minimum required to obtain bed motion
5. Run until stable bed forms develop

6. Terminate the run
7. Survey centerline of bed
8. Repeat steps 4-7, increasing depth by ($D_{84}/4$) until H/D84 = 1 is reached
9. Run water for average velocity profiles at H/D_{84} = 0.5 and H/D_{84} = 1.0, unless bed failed at H <= H/D_{84} = 1.0
10. Increase flow until bed fails (constant motion of D_{84} and of D_{max})
11. Repeat steps 1-10, at slopes of 5%, 7%, 9%, 12%.

Still photography was employed extensively, both digital and 35mm formats. It was found to be quite difficult to accurately capture the depth of the bed structure, but rulers and lighting were used in an attempt to be as descriptive as possible.

Sieve analyses were carried out at various stages of the testing, in order to sample the immobile portion of the bed, as well as the mobile portion of the bed. Some sieve analysis was conducted during the trial portion of the testing process, which resulted in bedload distribution, as well as stable bed size distribution.

4. **Results**

This section is divided into 2 parts. The first part describes in detail the scaling steps followed in this study.
The second part provides information about the flow, sediment transport, flow frictional, and bed form characteristics.

a. Development of the scaling methodology

To effectively translate the laboratory data into field parameters that are useful for design, it is necessary to imply the principles of similarity to the model design. Several general approaches to scaling can be found in the literature, and methods of scaling models are well-developed from years of practice. Typically, a hydraulic model is scaled based on known flow conditions at the prototype site, as well as desired prototype size (e.g., Parker et al., 1982). However, in this case, a more general approach is required, since the model will not be site-specific.

The Reynolds number, the ratio of inertial forces to viscous forces, is one of the dimensionless numbers governing similarity in fluid flows. However, when fully developed turbulence exists, as in the present study, viscous effects are small compared to turbulent effects, and can safely be ignored (Franzini et al., 1997).

In the present study, gravity is the main agent in determining the flow characteristics; this indicates that the Froude number is the parameter governing dynamic similarity (Franzini et al., 1997). For preservation of dynamic similarity, it is required that

$$\boldsymbol{F}_p = \boldsymbol{F}_m \qquad (11)$$

where the subscripts *p* and *m* denote prototype value and model value, respectively. The Froude number is the ratio of inertial forces to gravity forces, defined by

$$F_p = \frac{U_p}{\sqrt{g y_p}} \tag{12}$$

$$F_m = \frac{U_m}{\sqrt{g y_m}} \tag{13}$$

wherein *U* is the average depth velocity of the fluid, *g* is gravitational acceleration, and *y* is a characteristic length in the vertical direction. By combining (11), (12), and (13), after some manipulation it is obtained that

$$U_r = \sqrt{Y_r} \tag{14}$$

where the subscript *r* denotes the ratio of the prototype value to the model value for a particular parameter, as shown in (15) and (16), where Y_r is the ratio of vertical scales and Q_r is the ratio of flow-rates.

$$Y_r = \frac{Y_p}{Y_m} \tag{15}$$

$$Q_r = \frac{Q_p}{Q_m} \tag{16}$$

The continuity equation

$$Q_r = A_r U_r \tag{17}$$

can be combined with (16), leading to the following relationship (18):

$$U_r A_r = \frac{Q_p}{Q_m} \tag{18}$$

By combining (18) and (14) and recognizing that $A_r = X_r Y_r$, (19) is obtained.

$$\sqrt{Y_r} X_r Y_r = \frac{Q_p}{Q_m} \tag{19}$$

Finally, by combining (19) and (16) and solving for Y_r, the relationship in (20) is derived.

$$Y_r = \left(\frac{Q_r}{X_r} \right)^{2/3} \tag{20}$$

In this study, the flume width, as well as practical considerations of manageability, limits the diameter of the model culvert to 2.5 ft; the ratio of the prototype culvert diameter to that of the model yields the X_r ratio (21). Note that this horizontal scale ratio also applies to the length of the culvert.

$$X_r = \frac{X_p}{X_m} = \frac{\text{actual (field) culvert diameter}}{\text{Flume width}} \tag{21}$$

Since Q_r is known to be the ratio of the prototype flowrate and the flowrate available in the laboratory, it is now possible to solve for the vertical scale ratio Y_r. The ratio of the horizontal scale ratio to the vertical scale ratio is given by (22):

$$\delta = \frac{1}{S_r} = \frac{X_r}{Y_r} \tag{22}$$

where the parameter δ in (22) is known as the model distortion, which is due to the equality of vertical acceleration (gravity) in the Froude number. This must be limited in magnitude to

preserve similitude; a common limit of δ for mobile-bed models is 3 (Przedwojski et al., 1995), although large-scale studies have been performed using greater distortion factors (Peakall et al., 1996).

The above equations are applicable for scaling the culvert based on the flow discharge. Along the same lines, the sediment placed in a mobile-bed model must be scaled according to certain physical laws. The following method has been used successfully to scale river models, but care must be taken in the formulations. For the sediment the dimensionless parameter which must be identical in the model and prototype is the dimension-less bed shear stress parameter, expressed as the Shields parameters (Przedwojski et al., 1995),

$$\tau_m^* = \tau_p^* \tag{23}$$

where the Shields parameter is defined in (24).

$$\tau^* = \frac{\tau_o}{(\gamma_s - \gamma)\boldsymbol{D}} = \boldsymbol{idem} \tag{24}$$

In (24), γ is the specific weight of water, γ_s is the specific weight of the sediment, and $\tau_o = \gamma RS$ is the bed shear stress; other variables are as defined previously. The resulting combination of (23) and (24) is the following equality

$$\frac{\tau_{om}}{(\gamma_s - \gamma)_m \boldsymbol{D}_m} = \frac{\tau_{op}}{(\gamma_s - \gamma)_p \boldsymbol{D}_p} \tag{25}$$

$$\frac{(\gamma \boldsymbol{RS})_m}{(\gamma_s - \gamma)_m \boldsymbol{D}_m} = \frac{(\gamma \boldsymbol{RS})_p}{(\gamma_s - \gamma)_p \boldsymbol{D}_p} \tag{26}$$

Since water will be used in the model and prototype, some simplification is possible. If Γ_r is defined as the ratio of submerged particle weights (27),

$$\Gamma_r = \frac{(\gamma_s - \gamma)_p}{(\gamma_s - \gamma)_m} \tag{27}$$

then, the relationship (28) is derived by substituting scale ratios into (26),

$$\boldsymbol{R}_r \boldsymbol{S}_r = \Gamma_r \boldsymbol{D}_r \tag{28}$$

By again approximating the ratio of hydraulic radii of the prototype and model as the vertical scale ratio Y_r (Novak & Cabelka, 1981), the following result is apparent after eliminating this variable by combining (11) and (20):

$$\frac{U_p}{U_m} = \left(\frac{(\gamma_s - \gamma)_p D_p S_m}{(\gamma_s - \gamma)_m D_m S_p} \right)^{1/2} \tag{29}$$

By setting the ratio of submerged specific weights equal to (28), equation (29) can be rearranged to show that

$$S_r^{1/2} U_r = \Gamma_r^{1/2} D_r^{1/2} \tag{30}$$

Since the relative submergence can be shown, experimentally and theoretically, to be a significant parameter relating to incipient motion, it is desired to maintain its equality in the model and prototype. This can be written simply as

$$Y_r = D_r \tag{31}$$

To scale the model in a homogeneous manner, it is now necessary to fix several parameters. As steep slopes will be used in the prototype, it is unnecessary to distort the vertical scale, as is

typically done in large-scale models. Therefore, the vertical and horizontal scales will be equal in the model (no scale distortion). The following equations may be implied from this δ = 1:

$$X_r = Y_r \tag{31}$$

$$S_r = \frac{Y_r}{X_r} = 1 \tag{32}$$

It is desirable to use actual river rock in the model, as this is readily available in the wide size range necessary for the well-graded streambed; it is also noted that since large sizes will be used, cohesive behavior of the sediment will not be an issue. Setting Γ_r = 1 accomplishes this, and the model scaling is now complete, with respect to the dimensions and hydraulic characteristics of the model. The flowrate ratio is obtained by rewriting the continuity equation and manipulating variables. The result, finally, is that

$$Q_r = X_r Y_r^{3/2} \tag{33}$$

The Darcy-Weisbach friction factor is commonly used to express head losses in pipes, but it also can be used for open channel flows. The advantage of the Darcy friction factor is that it is dimensionless, and can be used with any dimensionally homogeneous system; this is not, however, true of the commonly used Manning's coefficient. To effectively use the friction factor measured in the model, it must be scaled up to the prototype, as outlined in

the following procedure. By writing the ratio of friction factors $f_r = f_p/f_m$ the following is evident:

$$f_r = \frac{\rho_p S_p U_m^2}{\rho_m S_m U_p^2} \qquad (34)$$

By recalling that the ratio of hydraulic radii may be considered equivalent to the vertical scale ratio, (34) is recast as

$$f_r = \frac{Y_r}{U_r^2} \qquad (35)$$

After combining (34) with (22) and simplifying, it becomes apparent that

$$f_r = 1 \qquad (36)$$

The implication of (35) is that for modeling purposes, the prototype friction factor will be identical to the model friction factor, providing the sediment used in each has an identical specific gravity.

Discussion

The purpose of this calculation exercise is twofold: it provides an estimate of the size of sediment which will be necessary for experiments, and demonstrates the application of scaling the model values up to prototype values. The prototype values of length, slope, and diameter are fixed, while the flowrate and sediment size are determined based on the selected model values. The benefit of this scaling procedure is that the slope ratio is 1:1, due to the small sediment size used; however, as stated previously, the hydraulically rough boundary must be enforced.

All results specified above are reasonable, in view of the parameters which are fixed. The flowrate is well within the capability of the laboratory pumps, and the slope will be easily established in the flume. Sediment used in the flume will be the same as that used in the field, but the flume will have increased slope to compensate for this distortion. Geometric distortion is within recommended limits, which indicates that the model should perform very well for this case.

b. Results for stability criteria, bed forms, frictional characteristics.

Figure 3 illustrates the dependence of the Shields parameter with respect to the Froude number. The results follow a similar trend (the fit line is almost parallel to that of Kilgore and Young) with the results reported by Kilgore and Young when D_{50} is used as the characteristic diameter in the Shields relation. Figure 3 is clearly shown that for Froude numbers greater than 0.7 the dimensionless critical stress is strongly dependent of the Froude number. In addition, Figure 3 shows that the Kilgore and Young method overestimates the value of the shear stress (for the reasons explained in the literature review section, aeration problems). In this study, the critical stress (when it is calculated as function of D_{84}) is found within the ranges reported in the literature (Abt et al. 1988; Bathurst et al. 1985). In this investigation, the upper limit for the dimension-less shear stress is 0.045 (when D_{84} is used). Figure 3 also shows that during the course of this study the flow was subcritical to

critical. This is consistent with the conclusion of Whittaker and Jaeggi (1982) who performed similar experiments. In very few cases the flow became supercritical, and when it did was marginally above the critical conditions.

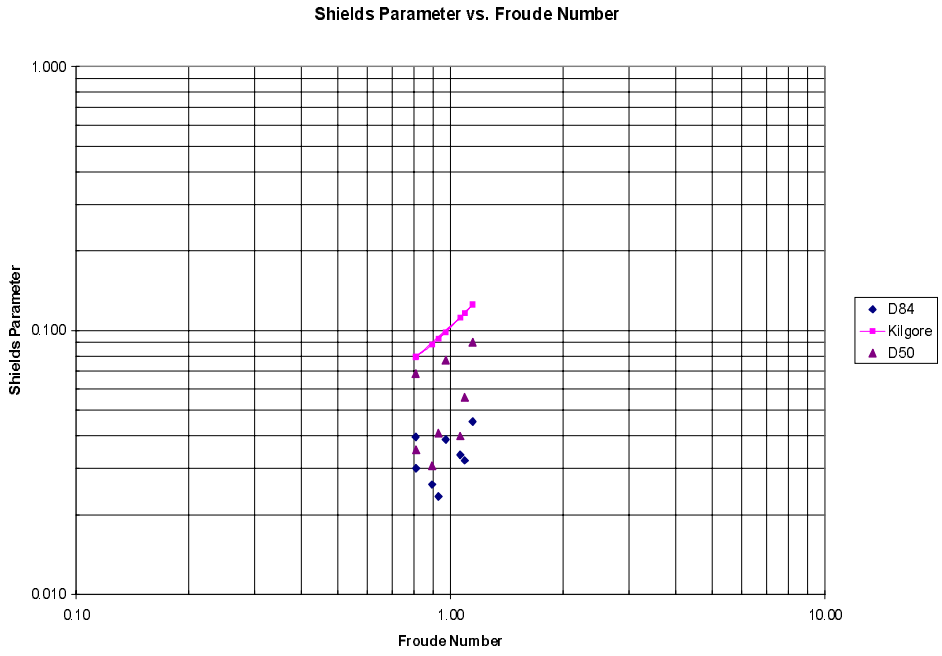

Figure 3: Variation of the Shields stress as function of the Froude number.

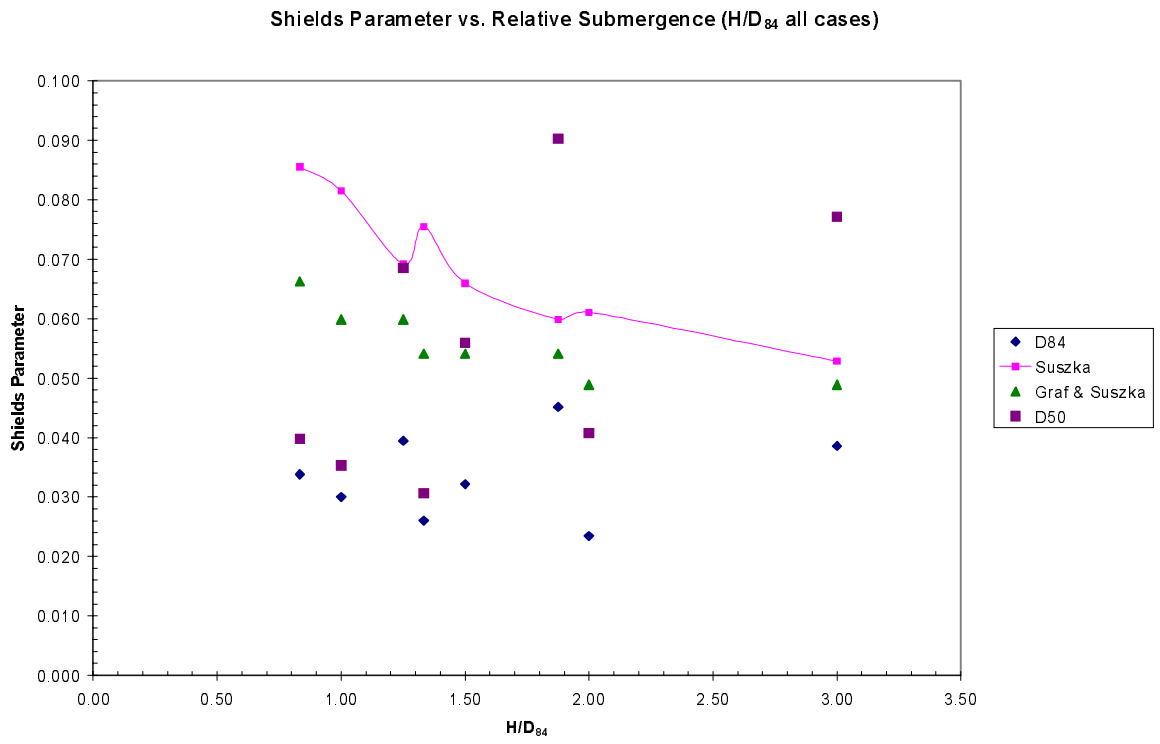

Figure 4. Variation of the Shields stress as function of the Relative submergence (H/D_{84}).

Figure 4 depicts the variation of the Shields parameter as function of the Relative submergence (H/D_{84}). The Suzka and Suzka and Graf data clearly show that as the relative submergence increases, the value of the stress reduces. In the study, it has been shown that that the bed shear stress is not strongly dependent of the H/D_{84} ratio. This differentiation can be explained by the fact that the Suzka study has been performed for small size particles (with diameter less than 4 mm). The above findings suggest that for large size particles (with diameter greater than 64 mm) the importance of the relative submergence minimizes.

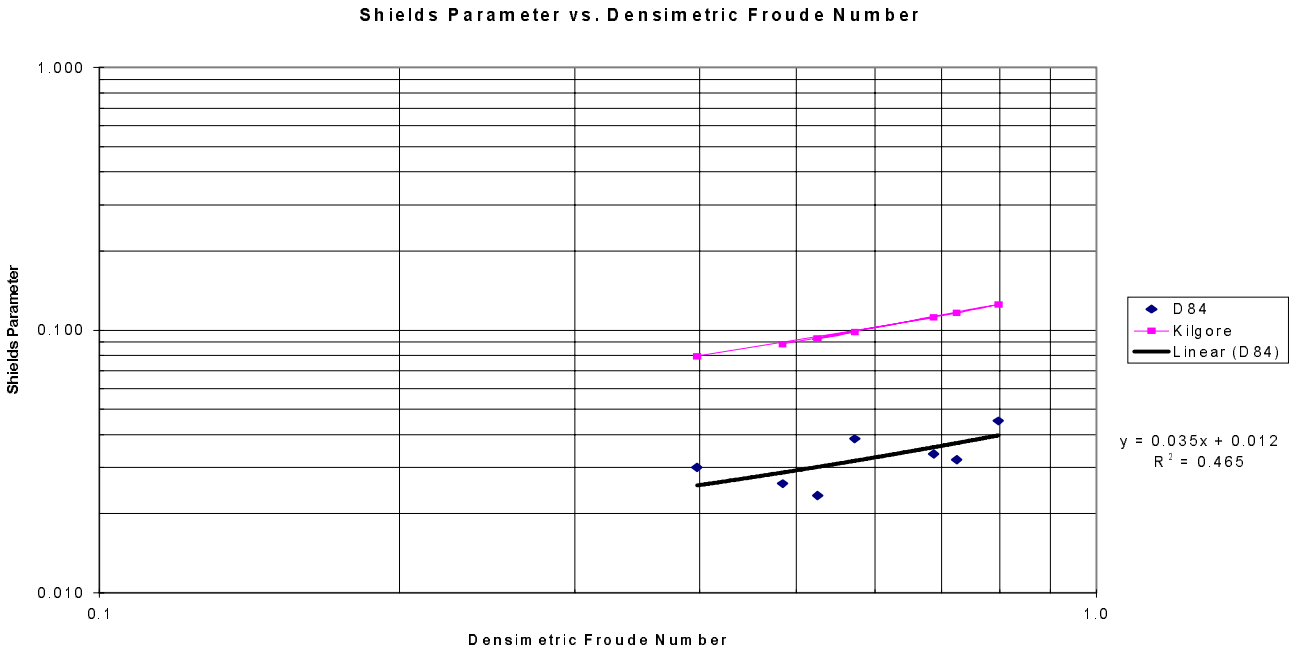

Figure 5. Variation of the Shields parameter with the densimetric Froude number.

Figure 5 shows the variation of the Shields parameter with the densimetric Froude number. Figure 5 exhibits the same behavior with that of figure 3, viz., increase of the Shields stress as the Froude number increases.

In figure 6 the variation of the critical unit discharge as function of slope S is provided. According to Buthurst et al. (1987) the critical unit discharge is defined as,

$$q_c = 0.21 S^{-1.12} \sqrt{g D_{16}^3} \qquad (37)$$

In the present study it appears to be more appropriate to express q_c as a function of D_{50} or D_{84} because these sizes are the controlling parameters affecting bed stability.

In figure 6 the vertical axis denotes the dimensionless unit discharge which is expressed as a fucntion of D_{50}. This figure provides a comparison between the Bathurst et al. method and the experimental results collected in this study. As it is shown in this fugure for slopes bewteen 3% and 4% the Bathurst et al. method underpredicts the erosion occurring. For slopes varying within the range of 4% to 10% our results appear to predict less erosion than the Bathurst et al. method. This deviation can be attributed to the fact that the Bathurst et al. data were primarily collected at the field and therefore erosion there appears to be dependent on other parameters such as bank erosion, large woody debris, sudden water rise, and possibly other parameters.

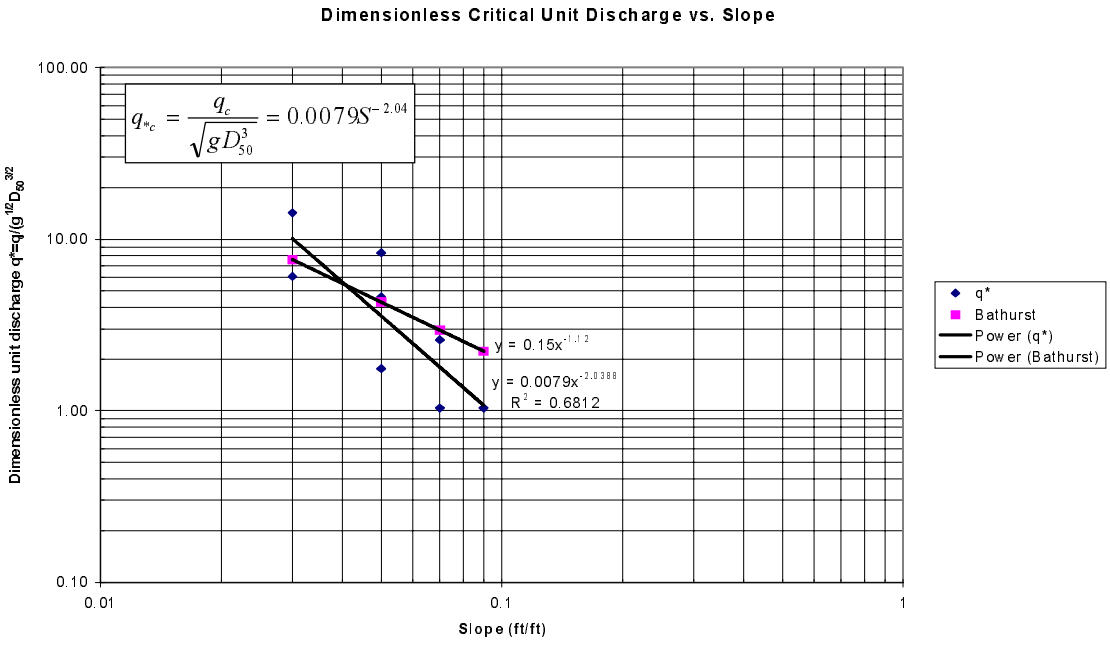

Figure 6. Variation of the dimension-less critical unit discharge as function of the Slope.

An outcome of this investigation is the derivation of an expression for the critical unit discharge,

$$q_c = 0.008 S^{-2.04} \sqrt{g D_{50}^3} \qquad (38)$$

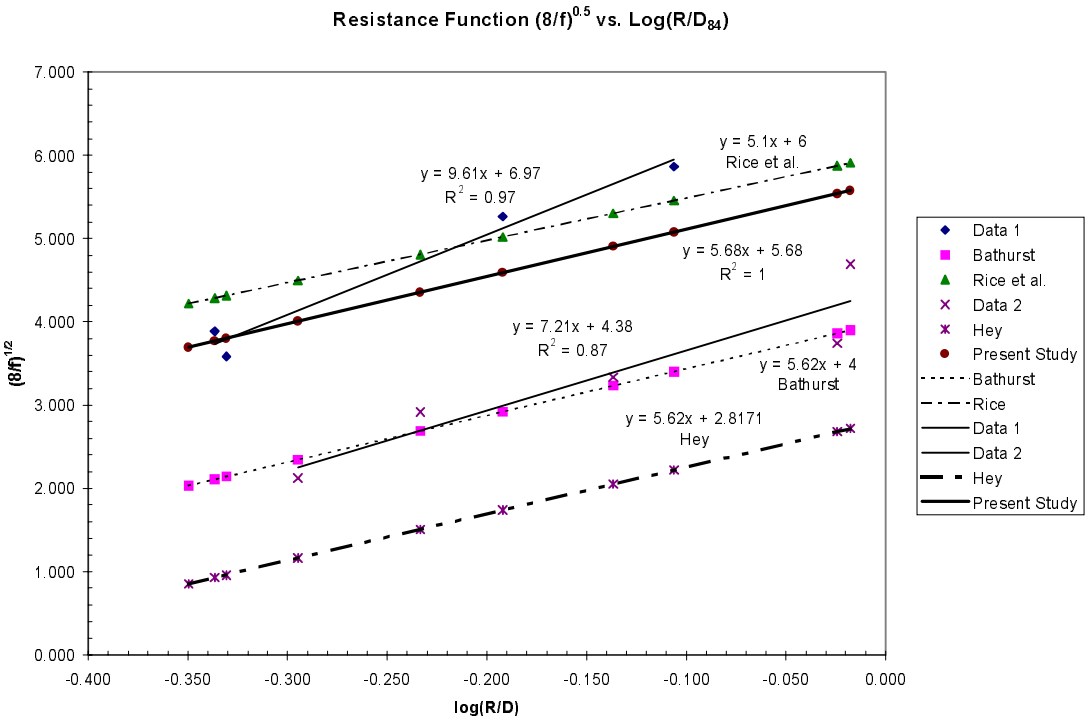

Figure 7. Resistance function versus relative submergence.

Figure 7 provides unique information about the resistance factor f. The friction factor is plotted as function of the hydraulic radious R and D_{84}. A comparison is provided by plotting the data of this study, the Hey data, the Bathurst et al. data, and the Rice et al. data. Figure 7 shows that the data collected here fall between the equations developed by Hey for small-scale roughness and by Rice et al. for loose riprap. In particular, there are 2 distinct trends that the data collected here appear

to follow. The data points that correspond to Froude numbers less than 0.8 seem to be well described by the Bathurst et al. formula. Instead, the data points corresponding to Froude number values greater than 0,8 are well represented by the Rice et al. formula.

Based on the above findings it is reasonable to propose use of a semilogarithmic equation that uses an average value for the intercept. By taking the arithmetic mean of the two experimental data fits, the intercept is 5.68. The final form of the equation developed here is:

$$\left(\frac{8}{f}\right)^{1/2} = 5.68\log\left(\frac{R}{D_{84}}\right) + 5.68 \qquad (39)$$

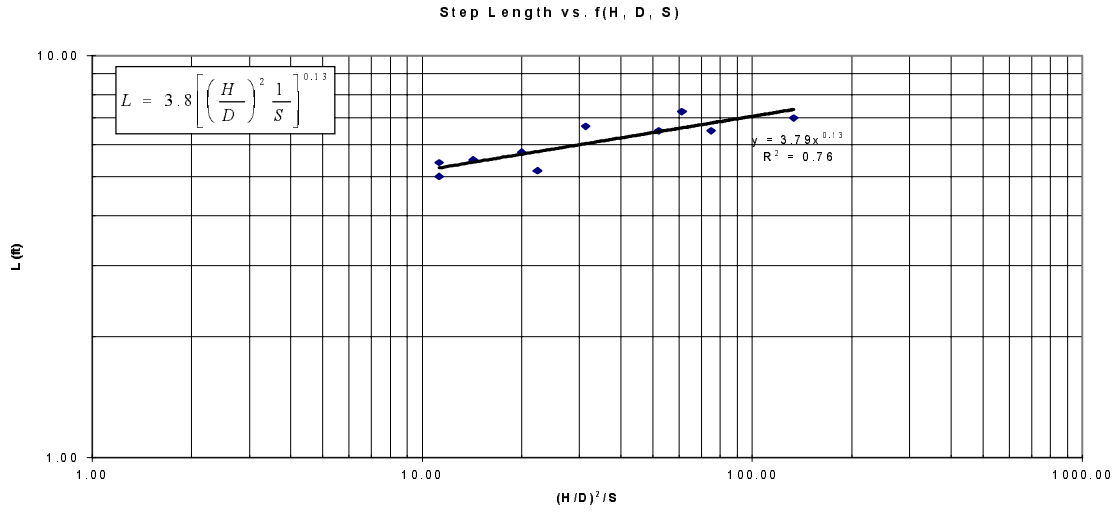

Figure 8. Step spacing in step-pool formations.

Figure 8 provides the spacing L (in ft) between two subsequent steps. The spacing L appears to be dependent of the average flow

depth, D_{84}, and slope. Instead Billi et al. (1998) have shown that the length L is only dependent of the slope.

A step-pool type morphology was most clearly evidenced in the high-slope (S>3%), high relative submergence tests. The term “dump deposit” used by Billi et al. seems to describe the structures formed in the low relative submergence tests (H/D < 1), particularly with the large bed size distributions. The dump deposits, or “heaps” are a cluster-type microform, imbricated above the rest of the bed. These are the beginnings of the step formations, and caused by shifting of a large ($<D_{84}$) particle until it is proud of the bed structure, or erosion along such a particle’s longitudinal boundaries. Smaller particles are typically deposited in the wake of this so-called “obstacle clast,” while other small particles are deposited upstream, as bedload can be locally obstructed by such a formation.

The plot shown in Figure 9 provides the maximum local scour depth (or equivalently maximum pool height) observed along the flume bed, as a function of flow parameters and sediment size distribution parameters. In order to construct Figure 9, extensive surveying was performed upon the termination of each test to measure the scaled scour hole size along the longitudinal direction of the flume. The maximum scour hole ($\mathbf{d}_{sm}$) was determined then by comparing the scour depth at several locations along the longitudinal direction of the flume.

The following data were collected from the tests:

- The volumetric discharge, **Q**
- The average flow depth during a test, **H**
- The mean size diameter from sieve analysis, $\mathbf{D_{50}}$
- The geometric standard deviation, $\sigma = (\frac{D_{84}}{D_{16}})^{0.5}$

The resulting data from all tests were dimensionlessly consolidated and the the scour depth was correlated to the discharge intensity, which is a modified Froude number expressed as, discharge intensity= $\frac{Q}{\sqrt{gH^5}}$

Analysis of the data yield the conclusion that the scour depth is function of the following dimensionless parameters: The ratio of mean size diameter and depth, $\frac{D_{50}}{H}$; the discharge intensity, $\frac{Q}{\sqrt{gH^5}}$; and the geometric standard deviation of the gravel bed, $\sigma = (\frac{D_{84}}{D_{16}})^{0.5}$. The geometric standard deviation value changes as the sediment bed composition changes.

Plotting the results as shown in Figure 9, a dimensionally homogeneous power equation was resulted that provides the scour depth d_{sm}:

$$\frac{d_{sm}}{H}\sigma^{0.25} = 0.35\left[\frac{Q}{\sqrt{gH^5}}\left(\frac{D_{50}}{H}\right)^{2.0}\right]^{0.18} \qquad (40)$$

This equation is useful for predicting scour depth for different gravel sizes under various flow conditions.

This can be used to determine a value for the step height desired in construction of a stable channel, and to determine whether the culvert will be scoured clean of bed material.

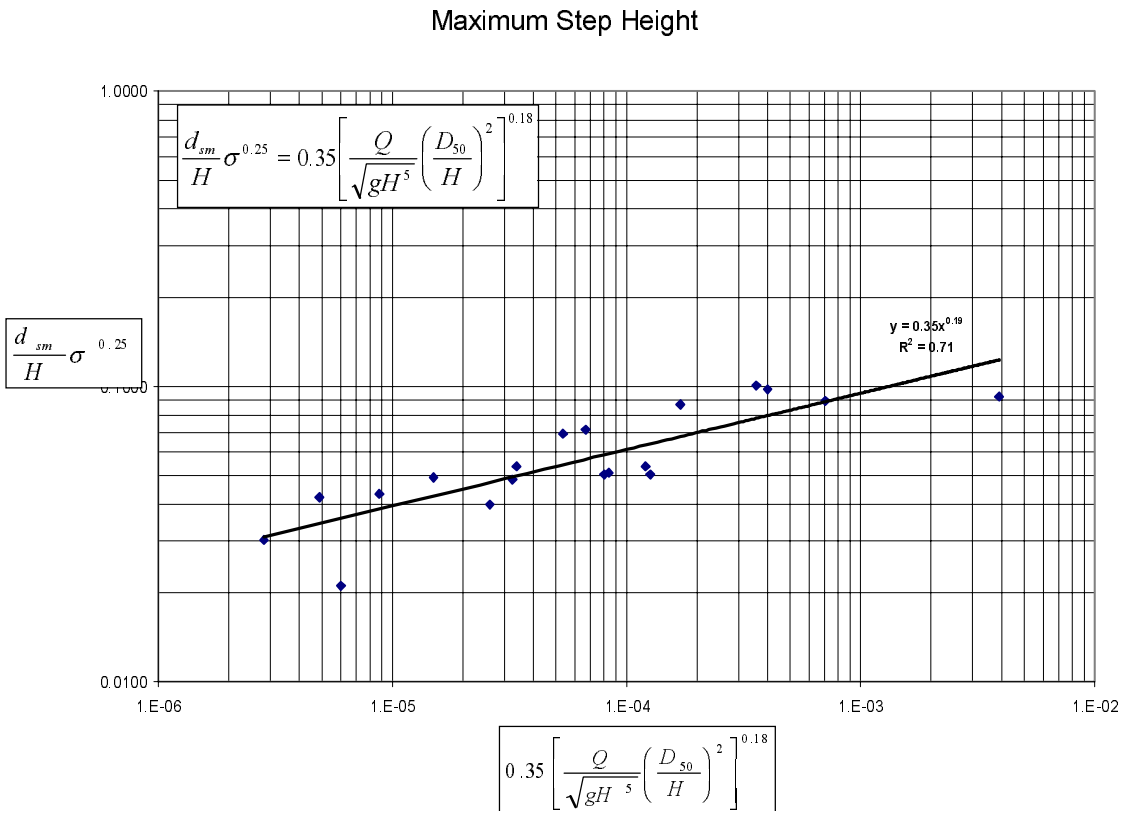

Figure 9. Pool height

Finally, Figure 10 illustrates the correction that was performed in order to obtain a correct value for the velocity from the Swoffer instrument. Due to the presence of significant surface waves, aeration was present during the tests. Also, it was observed that measurements performed atop a step present a higher degree of error than measurements performed within a pool. Similar observations were made by Bathurst et al. 1985 for measurements in natural streams. Bathurst et al. 1985 had to apply a similar technique.

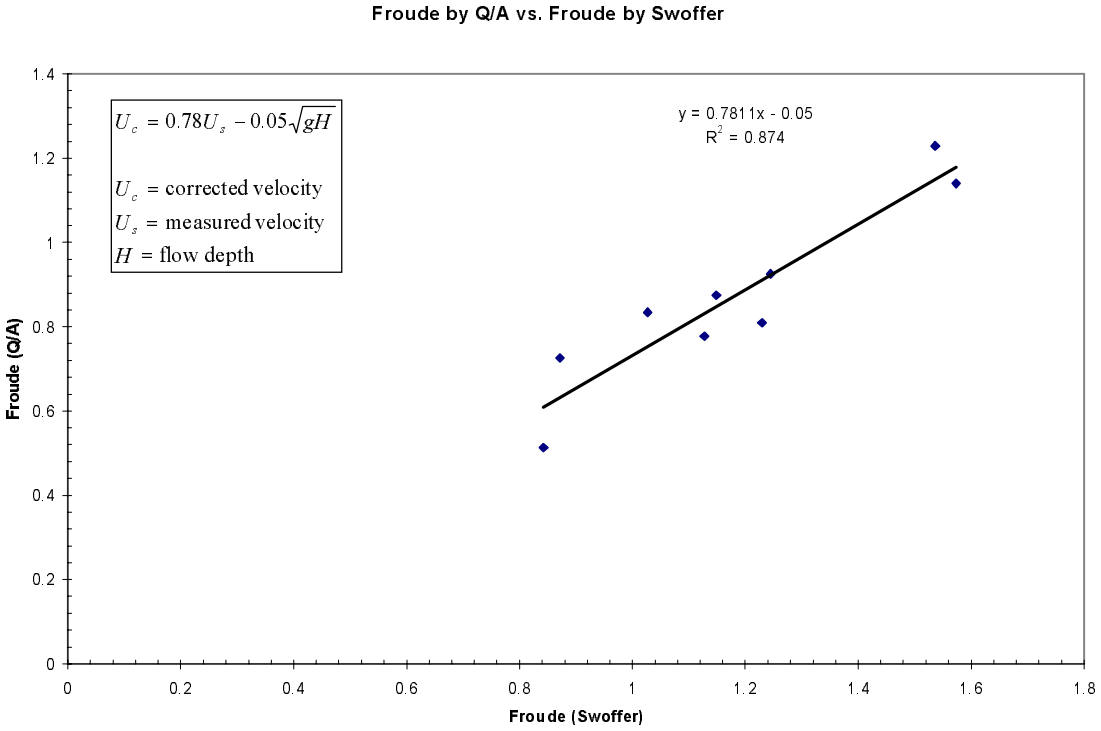

Figure 10: The correction equation applied to the swoffer measurements

Table 1 summarizes the flow parameters collected throughout this experimental work, such as Discharge, Depth, average depth velocity (Q/A), hydraulic radius, friction velocity, and EDF.

Table 1

Slope (ft/ft)	Q (cfs)	D84 (in)	H (in)	U (fps)	A (ft^2)	R (ft)	U(Q/A) (fps)	u* (fps)	t*	R*	U/u* N/A	H/D N/A	EDF (lb/ft-s)	f N/A
0.03	0.82	2	2.17	2.72	0.44	0.16	1.84	0.418	0.020	6.97E+04	6.508	1.09	3.40	0.363
0.03	2.36	4	3.91	4.03	0.8	0.26	2.95	0.561	0.018	1.87E+05	7.183	0.98	5.42	0.232
0.03	0.93	4	2	2.12	0.41	0.15	2.27	0.401	0.009	1.34E+05	5.284	0.5	4.18	0.223
0.05	2.73	4	5	4.99	1.02	0.32	2.67	0.819	0.038	2.73E+05	6.092	1.25	8.18	0.571
0.05	0.82	4	2.07	2.42	0.42	0.15	1.93	0.527	0.016	1.76E+05	4.592	0.52	5.93	0.529
0.07	4.71	6	5.13	5.7	1.05	0.32	4.48	0.982	0.036	4.91E+05	5.807	0.86	19.25	0.288
0.07	1.81	6	3.4	3.47	0.7	0.23	2.60	0.799	0.024	4.00E+05	4.342	0.57	11.16	0.623
0.07	1.81	4	3.58	3.81	0.73	0.24	2.47	0.820	0.038	2.73E+05	4.646	0.9	10.60	0.721
0.07	1.08	4	2.73	2.36	0.56	0.19	1.93	0.716	0.029	2.39E+05	3.296	0.68	8.29	0.942
0.07	1.24	6	3.77	2.68	0.77	0.25	1.61	0.842	0.027	4.21E+05	3.185	0.63	6.90	1.774

Figures 11(a)-(d) illustrate the longitudinal velocity for the three bed sizes.

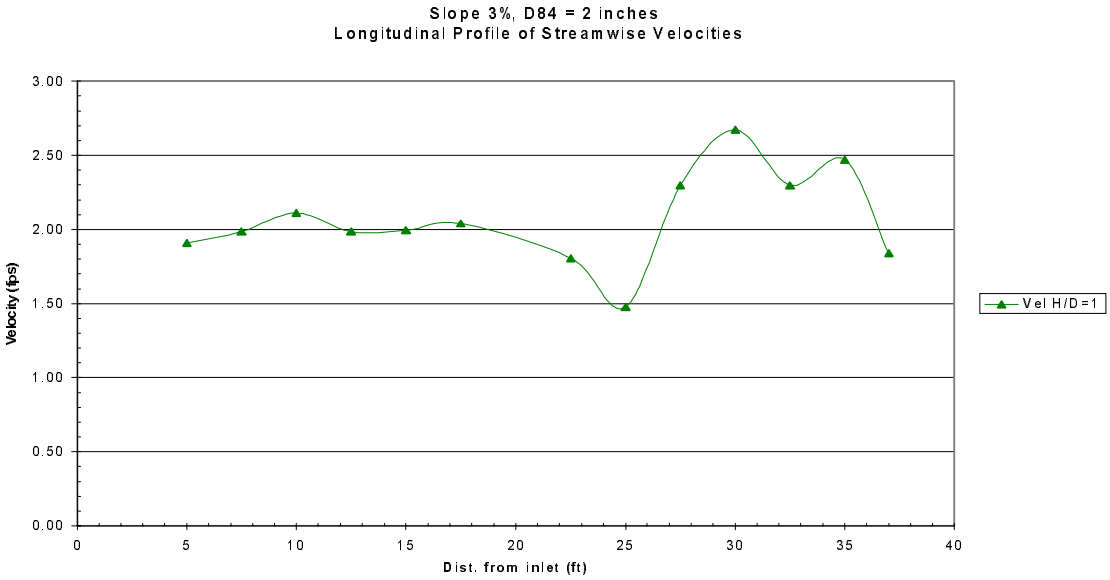

Figure 11(a). Longitudinal velocity

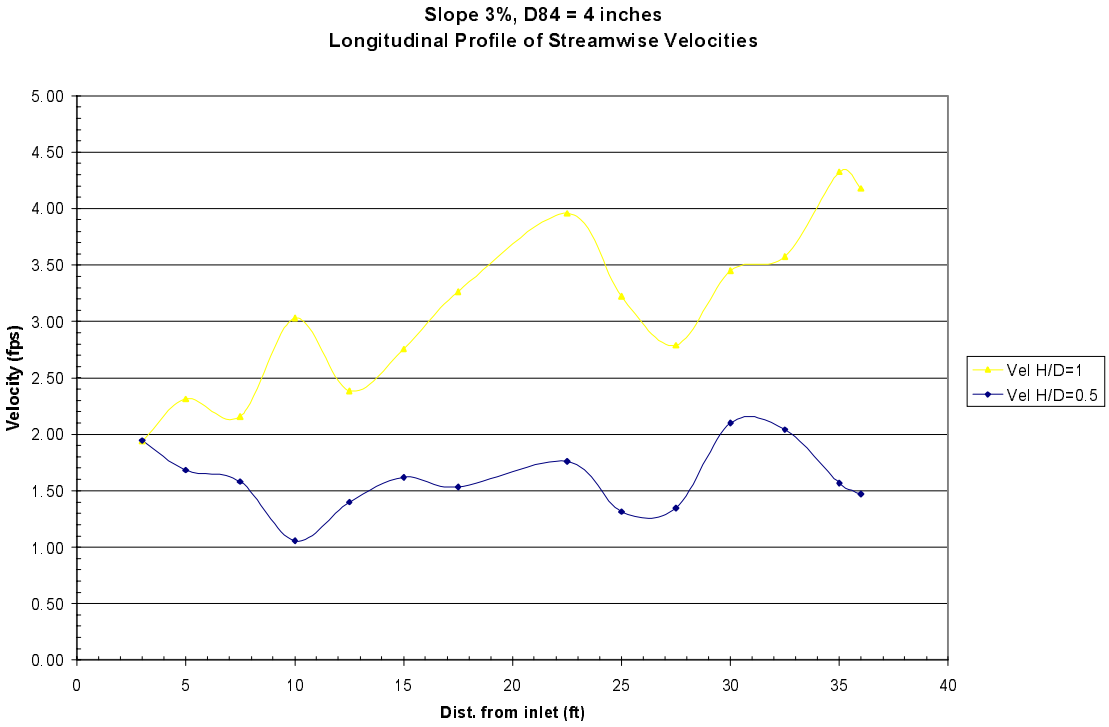

Figure 11(b). Longitudinal velocity

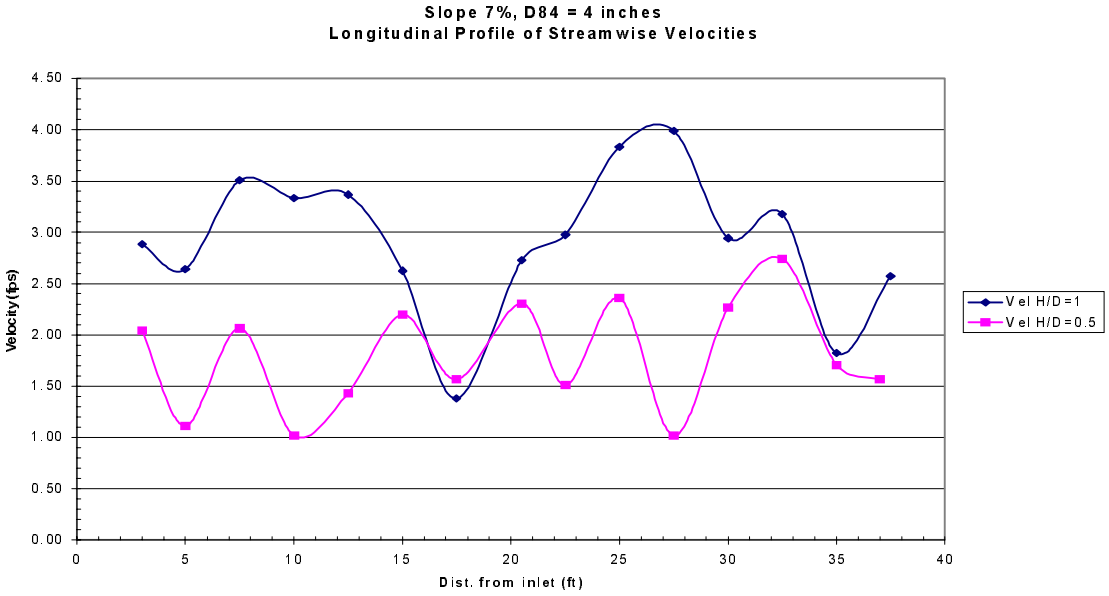

Figure 11(c).Longitudinal velocity

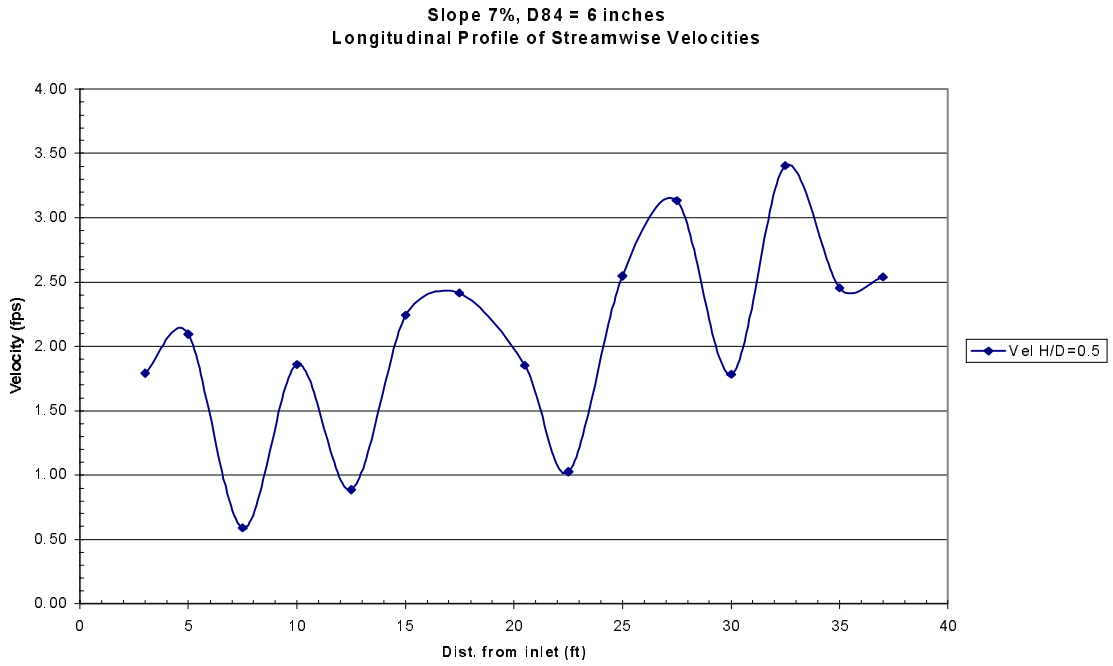

Figure 11(d). Longitudinal velocity

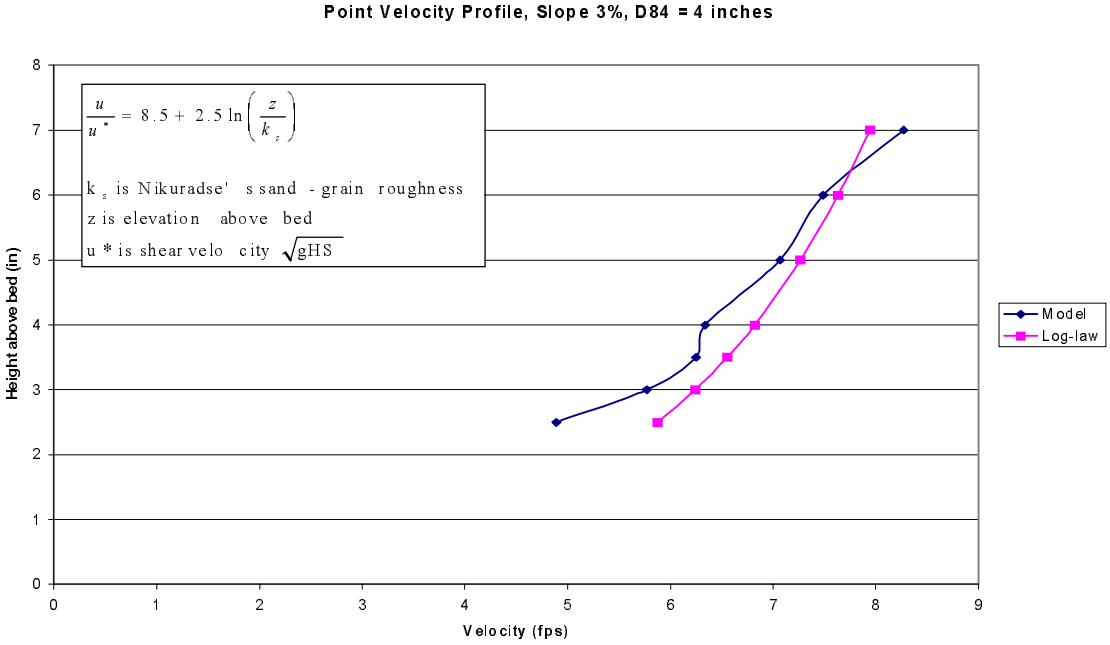

Figure 12. Logarithmic law profile

Figure 10 demonstrates the local mean velocity distribution along a vertical for the 3% slope. It is shown that the mean velocity although follows the shape of a log-profile is less in magnitude than the anticipated velocity distribution calculated via the log-law. The reason for that is found on the presence of a rough boundary and possibly on the location of the measurement points. Typically, in rough boundaries the mean velocities become less important with respect to magnitude. The most dominant parameters for rough boundaries are the so-called turbulent intensities (Nazu and Nakawaga 1993; Papanicolaou et al. 1999). Turbulent intensities show the deviation of the velocity from its mean value. A (turbulent) velocity (which is measured with a laser or acoustic Doppler) consists of two components: the mean component (that is measured via Nixon probe or a Swoffer, for example) and the fluctuating component that is actually the standard deviation of the turbulent velocity from the mean velocity. It has been shown (e.g., Nelson et al. 1995; Papanicolaou et al. 1999, 1997, 1995) that as the roughness increases (practically speaking as the diameter and compactness of sediment increases) turbulence becomes also important.

For step-pool formations measurements of turbulence do not exist in the literature. There are though measurements for sand bed forms (Best and Bennett 1997). For sand bed streams the measurements of turbulence indicate that within a pool two turbulent eddy structures are dominant, the inward and outward interactions. At the crest of dunes or antidunes, the dominant

events are: the sweeps and ejections. The sweeps and ejections cause respectively the action of drag and lift force. The outward and inward interactions do not have the capacity of transferring momentum from the water surface to the bottom of the stream. This is the reason that fish finds its resting areas within pools.

In the present study, since H/D_{84} was less than 1.0 turbulent measurements were not possible to be obtained with the acoustic Doppler. Another difficulty was the level of noise encountered during preliminary measurements. The presence of roughness of this size makes it impossible to collect turbulent measurements for $H/D_{84}<1$. However, based on preliminary observations of the PI of this project one can speculate the following:

1. The level of turbulence was higher for the largest size and less for the smallest size gravel tested here.
2. Although conclusion 1 holds in general true, one should note that the bed form configurations were pronounced for D_{84}=4 and 5 inches. Hence, pools and steps or mixed-structures is formed when the larger size gravel is present. Subsequently, habitat friendly geomorphologic conditions are formed when the larger size sediment is present.

3. Based on preliminary calculations of the PI the turbulent velocity can be at least 4-5 times greater than the mean velocity in water flows (Papanicolaou et al. 1999). This is the maximum value that turbulent velocities typically obtain. For this purpose, the designer should increase always the design parameters (critical stress) by a factor of 1.2.

c. Example-Tarboo Creek at Coyle Road:

Given:

Drainage Area: 0.85 sq mi

Design Flows: Q_{fp} = 12 cfs
Q_{25} = 75 cfs
Q_{100} = 100 cfs

Allowable Design Velocity: 4 fps

Stream Width at OHW = 9.4 feet

Existing Bed Material: D_{100} = 14"
D_{84} = 6"
D_{50} = 2.2"
D_{25} = 1.0"
D_{15} = 0.7"

Channel Slope 5%

Worked Example, Using Experimental Results/Solution:

1. Choose culvert width 12’ as first trial
2. Assume rectangular geometry for countersunk culvert (reasonable for low depths)
3. Solve for normal depth as follows:

$$f = \frac{8gRS}{U^2} = \frac{8gA^3S}{Q^2P}$$, where

g is gravitational acceleration
R is hydraulic radius
A is cross-sectional flow area
S is slope
Q is volumetric flowrate
P is wetted perimeter

Let depth of flow = *H* → *A* = 12*H* and *P* = *12* + 2*H*

$$f = \frac{8g(12H)^3 S}{Q^2(12+2H)}$$

From the curve-fit of the friction factor data:

$$\sqrt{\frac{8}{f}} = 5.7\left[\log\left(\frac{R}{D_{84}}\right)+1\right]$$

Substitute known values

$$\left[\frac{Q^2(12+2H)}{32.2(12)^3 H^3(0.05)}\right]^{1/2} = 5.7\left\{\log\left[\frac{12H}{(12+2H)\left(\frac{6}{12}\right)}\right]+1\right\}$$

Solving using a bisection algorithm (written in the C computer language)

Q = 12 cfs => H = 0.32 ft
Q = 75 cfs => H = 0.85 ft
Q = 100 cfs => H = 1.0 ft

4. Solve for depth-averaged velocities and Froude numbers for each case.

$$Q = UA \Rightarrow U = \frac{Q}{A}$$

$$\mathbf{F} = \frac{U}{\sqrt{gH}}$$

Q (cfs)	U (fps)	F
12	3.1	0.97
75	7.4	1.4
100	8.3	1.5

Comments: The Froude numbers are quite high, but the velocity in the 12 cfs case is below the permissible limit of 4 fps.

5. Stability Analysis

a. Shields parameter (at flood)

$$\tau^*_{cr} = \frac{RS}{1.65D_{84}} = \frac{\left(\frac{1(12)}{12+2(1)}\right)0.05}{1.65(0.5))} = 0.05$$

Comment: This value of 0.05 indicates incipient conditions are exceeded for the 84th percentile particle for these flow conditions. This is to be expected in the case of a 100-year flood, however.

b. Check stability by critical unit discharge method

$$\frac{q_c}{\sqrt{gD_{50}}} = 0.0079S^{-2.04}$$

$$q_c = \sqrt{32.2\left(\frac{2.2}{12}\right)^3}(0.0079)(0.05)^{-2.04}$$

q_c = 1.59 cfs/ft, which implies a total flowrate of 12(1.59) = 19 cfs will induce motion of the median particle size.

6. Bedform Characteristics (caused by flood)

a. Step length

$$L = 3.8\left[\left(\frac{H}{D}\right)^2 \frac{1}{S}\right]^{0.13}$$

Length of step is approximately 7 ft. peak-to-peak distance. Note that L is in feet – THIS EQUATION IS NOT DIMENSIONALLY HOMOGENEOUS, AS THE CONSTANT 3.8 HAS UNITS OF FEET.

b. Step height

$$\sigma = \sqrt{\frac{D_{84}}{D_{16}}} = 2.93$$

$$\frac{d_{sm}}{H}\sigma^{0.25} = 0.35\left[\frac{Q}{\sqrt{gH^5}}\left(\frac{D_{50}}{H}\right)^2\right]^{0.18}$$

$$\frac{d_{sm}}{1}2.93^{0.25} = 0.35\left[\frac{100}{\sqrt{32.2(1)^5}}\left(\frac{\left(\frac{2.2}{12}\right)}{1}\right)^2\right]^{0.18} \Rightarrow d_{sm} = 0.24\,\text{ft.}$$

If step construction is desired, to facilitate formation of stable bed conditions, step height should be approximately 3 inches.

NOTE: The equations used in the preceding exercise are dimensionally homogeneous, with the noted exception of the step length formula. As a consequence, consistent use of units is desirable throughout the entire process. Lengths (including particle diameter, where applicable) are most conveniently calculated in feet, flowrate in cfs, and velocities in fps.

REFERENCES:

Ashida, K., and Bayazit, M. (1973). "Initiation of motion and roughness of flows in steep channels." *Proceedings of the 15 th Congress of the International Association for Hydraulic Research,* Istanbul, Turkey, 1, 475-484.

Bathurst, J.C., Li, R-M., and Simons, D.B. (1979). "Hydraulics of mountain rivers." Report No. CER78-79JCB-RML-DBS55, Civil Engineering Department, Colorado State University, Fort Collins, Colorado.

Bathurst, J.C., Graf, W.H., and Cao, H.H. (1982). "Initiation of sediment transport in steep channels with coarse bed material." *Euromech 156 : Mechanics of Sediment Transport,* Istanbul, Turkey, 207-213.

Bettess, R. (1984). "Initiation of sediment transport in gravel streams." Proc. Instn. Civ. Engrs, Part 2,Technical Note 407, 77, 79-88.

Bathurst, J. C. (1985). "Flow Resistance Estimation in Mountain Rivers." J. Hyd. Engrg., ASCE, 111(4), 625-643.

Bathurst, J.C. Graf, W.H., and Cao, H.H. (1987). "Bed Load Discharge Equations for Steep Mountain Rivers." Sediment Transport in Gravel-bed Rivers, ed. C.R. Thorne et al., John Wiley & Sons, Ltd.

Billi, P., D'Agostino, V., Lenzi, M.A., and Marchi, L. (1998). "Bedload, Slope and Channel Processes in a High-Altitude Alpine Torrent." Gravel-Bed Rivers in the Environment, ed. P.C. Klingeman et al., Water Resources Publications, LLC, Highlands Ranch, CO

Cao, H.H. (1985). "Etude experimentale des ecoulement dans un canal a pente raide et avec lit a gravier." Thesis No. 589, Ecole Polytechnique Federale de Lausanne, Lausanne, Switzerland.

Chang, Howard (1998). "Fluvial Processes in River Engineering." Krieger, Malabar, Fl.

Coleman, N.L. (1967). "A theoretical and experimental study of drag and lift forces
acting on a sphere resting on a hypothetical stream bed." *Proceedings of the 12 th Congress of the International Association for Hydraulic Research*, Fort Collins, CO, Vol. 3, 185-192.

Fenton, J.D., and Abbott, J.E. (1977). "Initial movement of grains on a stream bed: The effect of relative protrusion."

Proceedings of the Royal Society of London, Series A, Vol.352, 523-537.

Franzini, J., Finnemore, E. J., Daugherty, R. (1997). "Fluid Mechanics With Engineering Applications." 9th ed., McGraw-Hill.

French, Richard (1985) "Open Channel Hydraulics." McGraw- Hill, New York.

Grant, G.E., Swanson, F.J., and Wolman, M.G. (1990). "Pattern and Origin of Stepped-Bed Morphology in High-Gradient Streams, Western Cascades, Oregon." Geol. Soc. Am. Bull., 102, 340-352

Graf, W.H. and Suszka, L. (1987). "Sediment Transport in Steep Channels." J. Hydroscience and Hydraulic Engrg., 5(1), 11-26.

Hey, R.D. (1979). "Flow Resistance in Gravel-Bed Rivers." J. Hyd. Div., ASCE, 105(HY4), 365-379

Jarrett, R.D. (1984). "Hydraulics of high-gradient streams." *Journal of Hydraulic Engineering*, 110(11), 1519-1539.

Kilgore, R.T. and Young, G.K. (1993). "Riprap Incipient Motion and Shields' Parameter." Proc. Nat'l Conf. on Hyd. Engrg., 1993, ASCE, New York, NY, 1552-1557

Li, C.H. (1965). "The criteria of threshold shearing stress and ripple formation (experimental results in glycerine flow)." Report No.70, Nanjin Hydraulic Research Institute (in Chinese).

Lopez, J.L. and Falcon, M.A. (1999). "Calculation of Bed Changes in Mountain Streams." J. Hyd. Engrg., ASCE, 125(3), 263-270

Mizuyama, T. (1977). "Bedload transport in steep channels." Ph.D Dissertation, Kyoto University, Kyoto, Japan.

Montgomery, D.R., and Buffington, J.M. (1993). "Channel Classification, Prediction of Channel Response and Assessment of Channel Conditions." *Rep. TFW-SH10-93-002*, Washington Department of Natural Resources, Olympia, WA

Nezu, I., and H. Nakagawa (1993). Turbulence in Open Channel Flow. IAHR, A. A. Balkema, Rotterdam.

Novak, P., Cabelka, J., (1981). "Models in Hydraulic Engineering." Pitman Advanced Publishing Program, Boston, London, Melbourne.

Papanicolaou, A. and P. Diplas. 1998. *Numerical Solution of a Non - Linear Model for Self -Weight Solids Settlement*. Journal of Applied Mathematical Modeling, Elsevier Science, Vol. 23, no. 5, pp. 345-36.

Papanicolaou, A., P. Diplas, M. Balakrishnan, and C.L. Dancey. 1999a. *Computer Vision Techniques for Sediment Transport*. Journal of Computing in Civil Engineering, ASCE, Vol. 13, no.2, pp. 71-79.

Papanicolaou, A., P. Diplas, M. Balakrishnan, and C.L. Dancey. 1999b. *The Role of Near-bed Turbulence Structure in the Inception of Sediment Motion*, accepted for publication to the Journal of Engineering Mechanics, ASCE.

Parker, G., Martinez, I., Hills, R. (1982). "Model Study of the Minnesota River Near Trunk Highway No. 169 Bridge, Minnesota." University of Minnesota, St. Anthony Falls Laboratory, Project Report No. 213.

Pazis, and Graf, W.H. (1977). "Erosion et deposition; un concept probabiliste." *Proceedings of the 17 th Congress of the International Association for Hydraulic Research*, Baden-Baden., Vol.1, 39-46.

Peakall, J., Ashworth, P., Best, J. (1996). "Physical Morphology in Fluvial Geomporphology: Principles, Applications and Unresolved Issues." Proc. 27th Binghamton Symposium in Geomorphology, John Wiley & Sons, Ltd.

Przedwojski, B., Blazejewski R., Pilarczyk, K. W., (1995) "River Training Techniques." A.A. Balkema, Rotterdam, Brookfield, Vt.

Rice, C. E., Kadavy, K. C., and Robinson, K. M. (1998). "Roughness of Loose Rock Riprap on Steep Slopes." J. Hyd. Engrg., ASCE, 124(2), 179-185.

Road Engineering Journal (1997). "Designing Highway Culverts That Do Not Impede the Movements of Resident Fish Species." TranSafety, Inc., [http://www.usroads.com/journals/p/rej/9711/re971102.h tm]

Sear, D.A. (1996). "Sediment Transport Processes in Pool-Riffle Sequences." *Earth Surface Processes and Landforms*, v. 21, 241-262

Suszka, L. (1991). "Modification of transport rate formula for steep channels." Lecture Notes in Earth Sciences, ed. A. Armanini and G. DiSilvio, Springer-Verlag, Berlin, 59-70

Wang, S. and Shen, H. (1985). "Incipient Motion and Riprap Design." J. Hyd. Engrg., ASCE, 111(3), 520-538

Tabata, S., and Ichinose, M. (1971). "An empirical study of critical tractive force of large gravel." The SHIN-SABO 79, May 1971.

Trieste, D.J. (1992). "Evaluation of supercritical / subcritical flows in high-gradient channel." *Journal of Hydraulic Engineering*, Vol.118, No.8, 1107-1118.

Wang, S.Y. (1975). "Stability of alluvial rivers." Technical Report, Tianjin University (in Chinese).

Wahl, K.L (1993). "Variation of Froude number with discharge for large-gradient streams." Hydraulic Engineering'93, 1517-1522.

Washington Dept. of Fish and Wildlife (1998). "Fish Passage Design at Road Culverts. WDFW, Habitat and Lands Program, Environmental Engineering Division

White, Dale (1996). "Hydraulic Performance of Countersunk Culverts in Oregon." Master's Thesis, Oregon State University

Wittler, R.J., and Abt, S.R. (1995). "Shields parameter in low submergence or steep flows." River, Coastal and Shoreline Protection : Erosion Control Using Riprap and Armourstone, Edited by C.R. Thorne, S.R. Abt, F.B.J Barends, S.T. Maynord and K.W. Pilarczyk. John Wiley & Sons Ltd., 93-101.

APPENDIX A

Figure A1. Side view of tilting flume, looking downstream (the flume is the structure at the left side of the image). The slope in the photo is approximately 0.07 ft/ft.

Figure A2. Top perspective of tilting flume (running diagonally across top of picture. Flume slope is 0.07 ft/ft.

Figure A3. Gravel bed (D_{84} = 4″) in place, looking downstream from culvert outlet. The V-notch weir used a water level control is visible at the tailgate of the flume, immediately preceding the sediment catchment system.

Figure A4. Gravel bed inside culvert, looking upstream. The Swoffer current meter is mounted on a rod in the center of the culvert. The D_{84} = 4″ gravel size distribution is shown here.

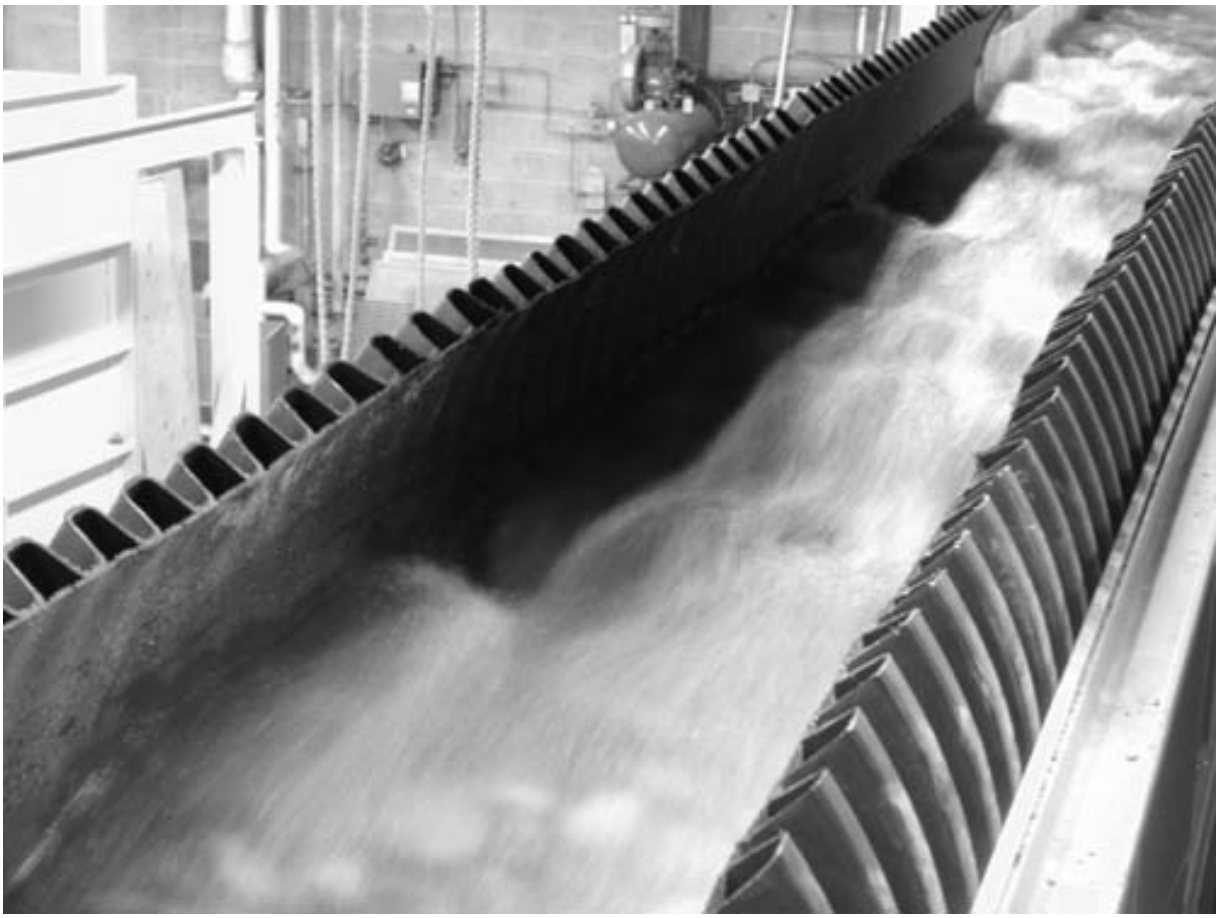

Figure A5. Time exposure of flow in the culvert, showing a typical step pattern formed in the bed.